ADAMS-BASHFORTH APPROXIMATIONS FOR DIGITAL CONTROL OF COMPLEX VEHICLE DYNAMICS

Mario Alberto Jordan and Jorge Luis Bustamante
Argentinean Institute of Oceanography (IADO-CONICET) and
Department of Electrical Engineering and Computers,
Universidad Nacional del Sur (DIEC-UNS).
Florida 8000 CCT, E1. B8000FWB Bahía Blanca, Argentina.
e-mail: mjordan@criba.edu.ar

Abstract

In this paper Adams-Bashforth approximations were employed for sampled-data modeling of a large class of vehicle dynamics in many degrees of freedom. The problem of path tracking and regulation with geometric and kinematic specifications on the reference paths was focused afterwards. An approach to model-based controller design was presented based on a Lyapunov method over an incremental functional of the path error energies. Asymptotic convergence for small sampling periods into a residual set with a measure depending only on the one-step-ahead sampled-data model errors was proved. Guidelines to select design matrices for independently tuning of the kinematic and geometric path tracking are provided. A case study for a 6 degrees-of-freedom vehicle illustrates the features of the proposed digital control system.

Key words

Vehicle dynamics, sampled-data models, nonlinear control, convergence, residual set.

1 Introduction

Although most research in control of nonlinear systems is devoted to systems in continuous time, the interest in the theory of discrete time models has been increasingly growing since most control applications are implemented digitally using sample and hold devices.

Physical models for the deterministic continuous-time nonlinear vehicle dynamics are typically available in the form of ordinary differential equations (ODEs), with eventually time-varying parameters. Translation of ODE-based descriptions to time-discrete models is an ineludible problem when applying digital technology to control system design. In the design of guidance systems for unmanned vehicles, most investigation is focused to continuous time controllers with a digitalization using the approximation of the time derivative according to the simplest numeric approach, the Euler's method [Cunha, Costa and Hsu, 1995; Smallwood and Whitcomb, 2003]. This generally provides a good control performance if motions are rather slow.

Improved technology in propulsion systems and ambitious requirements of accuracy on operations, make vehicles potentially more manoeuvrable and versatile so that the path tracking problem will impose more rapid changes of the variable involved. With this scenario in mind, it is conjectured here that more accurate and simple sampled-data models for control purposes of a complex nonlinear dynamics of the vehicle would have to be considered for achieving high control performance with feasible implementation in real time.

Many theoretical efforts are being focused to define sampled-data models for a broad class of nonlinear systems, see for instance [Albertos, 1996; Nešic, Teel and Sontag, 1999; Yuz and Goodwin, 2005]. Really, it is not possible to analytically describe the exact discrete-time model of the plant and so, in such situation, an approximate discrete-time model is the only alternative to use for controller design. Although a controller that stabilizes an approximate discrete-time system model for all small sampling periods is demanded, it could destabilize the exact discrete-time system model for all this small sampling periods [Nešic and Teel, 2004].

Traditional numeric methods arriving from simulation fields such as the Adams-Bashforth or Runge-Kutta methods [Hairer, Nørsett and Wanner, 1987], could be translated to one-step-ahead predictor for approximating exact discrete-time system model. The fact that local errors are always bounded if the ordinary differential equation is Lipschitz, even if the global error may be unbounded, make this approach very attractive for controller design purposes. Besides, *a-priori* seen, no significant restriction to the controller structure is required as for instance the demand of affine equations or polynomial structures. On the other side, they are very suitable in cases in which a physical ordinary differential equation of the system is available for controller design.

An open question to be explored yet is the adequacy

of numeric methods to complex dynamics in order for specific nonlinear controller design methods in the continuous time to be translated directly into the discrete-time domain with slight modifications. Besides, the roles played by the order of the approach and fast sampling rates on the model accuracy and stability of complex dynamics remain also open.

In this paper, the outstanding features of numeric methods will be exploited for modeling a large class of unmanned vehicles dynamics up to six degrees of freedom with model uncertainties. Specially the order of the approach and the sampling time will be investigated with focus on the behavior accuracy and till the stability implications in the path tracking problem. Some valuable guidelines are established for the employment of numeric methods with controller design purposes. Simulation results are presented to illustrate the features of the control approach developed.

2 Vehicle Dynamics

Many systems are described as the conjugation of two ODEs in generalized variables, namely one for the kinematics and the other one for the inertia. The block structure embraces a wide range of vehicle systems like mobile robots (MRs), unmanned aerial vehicles (UAVs), spacecraft and satellite systems (SSSs), autonomous underwater vehicles (AUVs) or remotely operated vehicles (ROVs), though with slight distinctive modifications in the structure among them.

Particularly, for underwater vehicles in six degrees of freedom (DOF) with cable connection to a mother ship (*i.e.*, for ROVs), the degree of interconnection among states is complex and involved, with accentuated influence of state-dependent Coriolis and centripetal, drag and cable forces. So we can say that the results developed here for the most complex case also will comprehend the more simple cases.

Let $\boldsymbol{\eta} = [x, y, z, \varphi, \theta, \psi]^T$ be the generalized position vector referred on an earth-fixed coordinate system termed O', with displacements x, y, z, and rotation angles φ, θ, ψ about these directions, respectively. Additionally let $\mathbf{v} = [u, v, w, p, q, r]^T$ be the generalized rate vector referred on a vehicle-fixed coordinate system termed O, oriented according to its main axes with translation rates u, v, w and angular rates p, q, r about these directions, respectively. The vector $\boldsymbol{\tau}$ is the generalized propulsion vector applied on O (also the future control action of a controller), $\boldsymbol{\tau}_c$ is a force perturbation applied on O (for instance the cable tug in ROVs), $\boldsymbol{\eta}_c$ is a perturbation of the position with respect to O', and finally $\mathbf{v}_c$ is a velocity perturbation with respect to O (for instance the fluid current in ROVs/AUVs or wind rate in UAVs).

The vehicle dynamics can be described by [Fossen, 1994]

$$\dot{\mathbf{v}} = M^{-1}\Big(-C(\mathbf{v})\mathbf{v} - D(|\mathbf{v}|)\mathbf{v} + \mathbf{g}(\boldsymbol{\eta}) + \boldsymbol{\tau}_c + \boldsymbol{\tau}\Big) \quad (1)$$

$$\dot{\boldsymbol{\eta}} = J(\boldsymbol{\eta})(\mathbf{v} + \mathbf{v}_c), \quad (2)$$

where M, C and D are the inertia, the Coriolis-centripetal and the drag matrices, respectively, $\mathbf{g}$ is the buoyancy vector and J is the rotation matrix expressing the transformation from the inertial frame to the vehicle-fixed frame. Finally, there may exist some perturbation $\boldsymbol{\tau}_c$ in the inertial system handled as an extra generalized force applied on O, for instance due to wind as in case of UAVs, fluid flow in AUVs, or cable tugs in ROVs.

As usually done, we will assume the thruster dynamics is parasitic when compared with the dominant vehicle dynamics. Besides, perturbations of the current and cable as in case of subaquatic vehicles are not considered here in the analysis, because their influences in the dynamics are quite similar to them of the model uncertainties considered in this work.

3 Discretization Method

The presence of zero-order holder in discrete control systems generally implies a delay of about one sampling period h at least, of the state/output with respect to the input. Thus, appropriate sampled-data models to control purposes require the ability to predict the actual state on the basis of samples related to past states and inputs. In other words, appropriate discretization methods are described by explicit algorithms in a nonautonomous form.

Let us investigate one important class of numeric method known as Adams-Bashforth approach [Butcher, 2003]. With the goal of implementing online control algorithms upon the sampled-data model we have to consider the particular explicit form and not the usually more accurate implicit form of the Adams-Bashforth. Moreover, in comparison with the Runge-Kutta methods, Adams-Bashforth methods do not use intersampling which make it adequate for control and identification purposes.

Generally speaking, series-based approximations of order p attempt to bring the local error to be

$$\mathbf{x}_{t_{n+1}} - \mathbf{x}_{n+1} = \boldsymbol{\varepsilon}_{n+1} \in \mathcal{O}(h^{p+1}), \quad (3)$$

where $\mathbf{x}_{t_{n+1}}$ is the sample at discrete time t_{n+1} of the state vector of a system $\dot{\mathbf{x}} = \mathbf{F}(\mathbf{x},\mathbf{u})$ with $\mathbf{F}$ Lipschitz and $\mathbf{u}$ the system input. The samples $\mathbf{x}_{t_{n+1}}$ of the system are referred to as the exact sampled-data model of the system, often an inexistent one in terms of model structure. On the other side, $\mathbf{x}_{n+1}$ is a prediction of the sampled-data model, $\boldsymbol{\varepsilon}_{n+1}$ the prediction error and $\mathcal{O}$ is the order function expressing that the local error is of an order of magnitude equal to a desired order of accuracy p with h the sampling period. Here, there is supposed the structure of the ODE in $\mathbf{F}$ is known beforehand and the samples $\mathbf{x}_{t_{n+1}}$ are noiseless.

Particularly the Adams-Bashforth method is an explicit multistep linear method that performs an approximation of $\mathbf{x}_t$ with initial value $\mathbf{x}_{t_0}$ at $t = t_{n+1} = t_0 + (n+1)h$ with $n = 0, 1, 2, ...$ based on a linear combination of samples $\mathbf{F}(\mathbf{x}_{t_i},\mathbf{u}_{t_i})$ from $i = n$ up to $i = n - s + 1$, with s the so-called order of the approximation.

The coefficients of the linear combination are obtained by using the Lagrange formula for polynomial interpolation, which is locally a good approximation of the right-hand side of the differential equation that is to be solved. Accordingly, one achieves for different orders s the one-step-ahead prediction $\mathbf{x}_{n+1}$

$$s{=}1{:}\ \mathbf{x}_{n+1}{=}\mathbf{x}_n{+}h\mathbf{F}(\mathbf{x}_n,\mathbf{u}_n) \quad (4)$$

$$s{=}2{:}\ \mathbf{x}_{n+1}{=}\mathbf{x}_n{+}\frac{3h}{2}\mathbf{F}(\mathbf{x}_n,\mathbf{u}_n){-}\frac{h}{2}\mathbf{F}(\mathbf{x}_{n-1},\mathbf{u}_{n-1}) \quad (5)$$

$$s{=}3{:}\ \mathbf{x}_{n+1}{=}\mathbf{x}_n{+}\frac{23h}{12}\mathbf{F}(\mathbf{x}_n,\mathbf{u}_n){-}\frac{4h}{3}\mathbf{F}(\mathbf{x}_{n-1},\mathbf{u}_{n-1}){+}$$
$$+\frac{5h}{12}\mathbf{F}(\mathbf{x}_{n-2},\mathbf{u}_{n-2}) \quad (6)$$

$$s{=}4{:}\ \mathbf{x}_{n+1}{=}\mathbf{x}_n{+}\frac{55h}{24}\mathbf{F}(\mathbf{x}_n,\mathbf{u}_n){-}\frac{59h}{24}\mathbf{F}(\mathbf{x}_{n-1},\mathbf{u}_{n-1}){+}$$
$$+\frac{37h}{24}\mathbf{F}(\mathbf{x}_{n-2},\mathbf{u}_{n-2}){-}\frac{9h}{24}\mathbf{F}(\mathbf{x}_{n-3},\mathbf{u}_{n-3}). \quad (7)$$

For explicit Adams-Bashforth methods, the order of accuracy is equal to s, *i.e.*, $\mathbf{x}_{t_{n+1}} - \mathbf{x}_{n+1}{=}\boldsymbol{\varepsilon}_{n+1} \in \mathcal{O}(h^s)$.

Clearly, from (4)-(7), if $\mathbf{x}_n$, $\mathbf{x}_{n-1}$,... and $\mathbf{u}_n$, $\mathbf{u}_{n-1}$,... are system measures, it is $\mathbf{x}_{t_n}$, $\mathbf{x}_{t_{n-1}}$,... and $\mathbf{u}_{t_n}$, $\mathbf{u}_{t_{n-1}}$,... and $\mathbf{F}$ is Lipschitz, the samples, the prediction $\mathbf{x}_{n+1}$ as well as the local error $\boldsymbol{\varepsilon}_{n+1}$ yield bounded too. Besides, $\mathbf{x}_n \to \mathbf{x}_{t_n}$ for $h \to 0$.

4 Adams-Bashforth Sampled-Data Model for a Vehicle

Now using (1)-(2), it is valid in compact form

$$\dot{\mathbf{v}} = \mathbf{G}(\boldsymbol{\eta},\mathbf{v}){+}M^{-1}(\boldsymbol{\tau}{+}\boldsymbol{\tau}_c) \quad (8)$$

$$\dot{\boldsymbol{\eta}} = \mathbf{H}(\boldsymbol{\eta},\mathbf{v}{+}\mathbf{v}_c) \quad (9)$$

where the vector functions $\mathbf{G}$ and $\mathbf{H}$ are valuable expressions specified in the right members of (1) and (2), respectively, for the continuous-time model with known $\boldsymbol{\eta}$ and $\mathbf{v}$, cable and flow perturbations $\boldsymbol{\tau}_c$ and $\mathbf{v}_c$, and control action on the thrust $\boldsymbol{\tau}$.

Let us regard the Adams-Bashforth approximation of order s in the estimation form for the ODE system (1)-(2). Hence, it is valid

$$\mathbf{v}_{n+1} = \mathbf{v}_{t_n}{+}a_1\left(\mathbf{G}_{t_n}{+}M^{-1}\boldsymbol{\tau}_n\right){+}... + \quad (10)$$
$$+a_s\left(\mathbf{G}_{t_{n-s+1}}{+}M^{-1}\boldsymbol{\tau}_{n-s+1}\right)$$

$$\boldsymbol{\eta}_{n+1} = \boldsymbol{\eta}_{t_n}{+}b_1\mathbf{H}_{t_n} + ... + b_s\mathbf{H}_{t_{n-s+1}}, \quad (11)$$

where a_i and b_i are associated coefficients to the s-order approximation according to (4)-(7), $\mathbf{G}_{t_n}$ and $\mathbf{H}_{t_n}$. It is noticing that the predictor (10)-(11) is fed with exact samples of the continuous-time behavior. Moreover, the control action $\boldsymbol{\tau}$ is retained one sampling period h by a sample and holder, so, it is valid $\boldsymbol{\tau}_n = \boldsymbol{\tau}_{t_n}$, it means that there is a sample and, at the same time, an input of the sampled-data model.

For any digital controller design a known sampled-data model of the system is necessary. Though the model looks awkward to deal with, above all for large order s, the sampled-data model is modularly composed by delayed terms as indicated in (10)-(11). This modularity could be exploited in future designs of controllers.

In the following we illustrate results from a case study by means of numeric simulations of the open-loop continuous-time system (1)-(2) for a full-actuated ROV in 6 DOF along a quasi helicoidal path (see [Jordán and Bustamante, 2008]). In this way local and global errors originated in the sampled-data models (4)-(7) with respect to the exact sampled-data behavior for different sampling periods h and orders are compared and listed in Table I. The Comparison of the Adams-Bashforth method with another approximations in the form of interpolation approaches and black box models for control-system design purposes is presented in [Jordán and Bustamante, 2009].

The sampled-data model (10)-(11) contains the physical matrices. If they are completely known, this model can be applied to digital controller design. In case the physical matrices are not available, identification methods may be technically feasible to provide a model from sampled data despite the lack of parsimony. The proposition and evaluation of estimation methods fall outside the paper and is a goal of future research.

Table I - Influence of the sampling period and model order on the local error ε and global error ϵ for a vehicle in 6-DOF navigation in open loop along a helix

	$h = 0.01(s)$			
s	1	2	3	4
ε_{η_n}	$3.687.10^{-9}$	$3.829.10^{-11}$	$8.303.10^{-15}$	$9.178.10^{-15}$
ε_{v_n}	$5.564.10^{-8}$	$1.722.10^{-10}$	$9.153.10^{-11}$	$2.858.10^{-10}$
ϵ_η	$9.672.10^{-0}$	$5.000.10^{-3}$	$7.086.10^{-6}$	$8.840.10^{-6}$
ϵ_v	$4.083.10^{-1}$	$3.070.10^{-2}$	$3.251.10^{-5}$	$3.599.10^{-5}$
	$h = 0.05(s)$			
s	1	2	3	4
ε_{η_n}	$2.299.10^{-6}$	$6.162.10^{-8}$	$1.745.10^{-9}$	$9.802.10^{-11}$
ε_{v_n}	$3.513.10^{-5}$	$9.138.10^{-7}$	$4.455.10^{-8}$	$4.285.10^{-8}$
ϵ_η	$8.552.10^{2}$	$1.081.10^{-1}$	$7.820.10^{-2}$	$1.600.10^{-3}$
ϵ_v	$0.4083.10^{2}$	$2.390.10^{-1}$	$4.860.10^{-2}$	$2.28..10^{-2}$
	$h = 0.1(s)$			
s	1	2	3	4
ε_{η_n}	$3.657.10^{-5}$	$3.641.10^{-6}$	$4.311.10^{-7}$	$6.352.10^{-8}$
ε_{v_n}	$5.770.10^{-4}$	$5.797.10^{-5}$	$7.634.10^{-6}$	$2.428.10^{-6}$
ϵ_η	*unstable*	$6.018.10^{-0}$	$2.283.10^{-0}$	$1.820.10^{-1}$
ϵ_v	*unstable*	$3.519.10^{-1}$	$1.740.10^{-1}$	$2.169.10^{-1}$
	$h = 0.5(s)$			
s	1	2	3	4
ε_{η_n}	$1.880.10^{-2}$	$3.530.10^{-2}$	$7.460.10^{-2}$	$1.685.10^{-1}$
ε_{v_n}	$4.318.10^{-1}$	$1.123.10^{-0}$	$1.148.10^{-0}$	$2.628.10^{-0}$
ϵ_η	*unstable*	*unstable*	*unstable*	*unstable*
ϵ_v	*unstable*	*unstable*	*unstable*	*unstable*

5 Design of a Digital Controller for Path Tracking

We are able now to design specific digital controllers based on Lyapunov functions. To this end, let us suppose the interest lies on the path tracking of geometric and kinematic reference trajectories in discrete-time form specified as $\boldsymbol{\eta}_{r_{t_n}}$ and $\mathbf{v}_{r_{t_n}}$, respectively. We then define the exact sampled path errors as

$$\overset{\frown}{\boldsymbol{\eta}}_{t_n} = \boldsymbol{\eta}_{t_n} - \boldsymbol{\eta}_{r_{t_n}} \tag{12}$$

$$\overset{\frown}{\mathbf{v}}_{t_n} = \mathbf{v}_{t_n} - J_{t_n}^{-1}\dot{\boldsymbol{\eta}}_{r_{t_n}} + J_{t_n}^{-1}K_p\overset{\frown}{\boldsymbol{\eta}}_{t_n}. \tag{13}$$

where $K_p = K_p^T \geq 0$ is a gain matrix affecting the geometric path error and $J_{t_n}^{-1}$ means $J^{-1}(\boldsymbol{\eta}_{t_n})$. Clearly, if $\overset{\frown}{\boldsymbol{\eta}}_{t_n} \equiv \mathbf{0}$, then by (13) and (2), it yields $\mathbf{v}_{t_n} - \mathbf{v}_{r_{t_n}} \equiv \mathbf{0}$.

Let us consider errors of the sampled-data model predictions

$$\boldsymbol{\varepsilon}_{\eta_n} = \boldsymbol{\eta}_{t_n} - \boldsymbol{\eta}_n \tag{14}$$

$$\boldsymbol{\varepsilon}_{v_n} = \mathbf{v}_{t_n} - \mathbf{v}_n. \tag{15}$$

A one-step-ahead prediction is supported by the sampled-data model (10)-(11). So it is valid

$$\begin{aligned}\overset{\frown}{\boldsymbol{\eta}}_{t_{n+1}} = {} & \overset{\frown}{\boldsymbol{\eta}}_{t_n} + \\ & + b_1 J_{t_n}\left[\overset{\frown}{\mathbf{v}}_{t_n} + J_{t_n}^{-1}\dot{\boldsymbol{\eta}}_{r_{t_n}} - J_{t_n}^{-1}K_p\overset{\frown}{\boldsymbol{\eta}}_{t_n}\right] + \\ & + \sum_{i=2}^{s} b_i J_{t_{n-i+1}}\mathbf{v}_{t_{n-i+1}} + \boldsymbol{\eta}_{r_{t_n}} - \boldsymbol{\eta}_{r_{t_{n+1}}} + \boldsymbol{\varepsilon}_{\eta_{n+1}}\end{aligned} \tag{16}$$

$$\begin{aligned}\overset{\frown}{\mathbf{v}}_{t_{n+1}} = {} & \overset{\frown}{\mathbf{v}}_{t_n} + \\ & + J_{t_n}^{-1}\dot{\boldsymbol{\eta}}_{r_{t_n}} - J_{t_n}^{-1}K_p\overset{\frown}{\boldsymbol{\eta}}_{t_n} - J_{t_{n+1}}^{-1}\dot{\boldsymbol{\eta}}_{r_{t_{n+1}}} + J_{t_{n+1}}^{-1}K_p\overset{\frown}{\boldsymbol{\eta}}_{t_{n+1}} + \\ & + \sum_{i=1}^{s} a_s\left(\mathbf{G}_{t_{n-i+1}} + M^{-1}\boldsymbol{\tau}_{n-i+1}\right) + \boldsymbol{\varepsilon}_{v_{n+1}},\end{aligned} \tag{17}$$

where $\boldsymbol{\tau}_n$ is the unknown for controller design and $\boldsymbol{\varepsilon}_{\eta_{n+1}}$ and $\boldsymbol{\varepsilon}_{v_{n+1}}$ are the uncertainties of the model-based prediction.

We now define a cost functional of the path error energy

$$Q_{t_n} = \overset{\frown}{\boldsymbol{\eta}}_{t_n}^T\overset{\frown}{\boldsymbol{\eta}}_{t_n} + \overset{\frown}{\mathbf{v}}_{t_n}^T\overset{\frown}{\mathbf{v}}_{t_n}, \tag{18}$$

which is a positive definite and radially unbounded function in the error vector space. We will then design a digital state feedback for the path tracking problem for a vehicle system dynamics and afterward search for conditions to ensure the regulation of Q_{t_n} about zero as t_n tends to infinity.

The controller design will be carried out by establishing the incremental value of Q at t_{n+1} when only predictions $\boldsymbol{\eta}_{n+1}$ and $\mathbf{v}_{n+1}$ are available and $\boldsymbol{\tau}_n$ is the unknown control action. Thus, using (18) and (16)-(17) one gets

$$\begin{aligned}\Delta Q_{t_n} = {} & Q_{t_{n+1}} - Q_{t_n} = \\ & \left[\left(I - b_1K_p\right)\overset{\frown}{\boldsymbol{\eta}}_{t_n} + b_1\left(J_{t_n}\overset{\frown}{\mathbf{v}}_{t_n} + \dot{\boldsymbol{\eta}}_{r_{t_n}}\right) + \right. \\ & \left. + \sum_{i=2}^{s} b_i J_{t_{n-i+1}}\mathbf{v}_{t_{n-i+1}} + \boldsymbol{\eta}_{r_{t_n}} - \boldsymbol{\eta}_{r_{t_{n+1}}} + \boldsymbol{\varepsilon}_{\eta_{n+1}}\right]^2 - \\ & - \overset{\frown}{\boldsymbol{\eta}}_{t_n}^T\overset{\frown}{\boldsymbol{\eta}}_{t_n} + \\ & + \left[\overset{\frown}{\mathbf{v}}_{t_n} + J_{t_n}^{-1}\dot{\boldsymbol{\eta}}_{r_{t_n}} - J_{t_n}^{-1}K_p\overset{\frown}{\boldsymbol{\eta}}_{t_n} - \right. \\ & - J_{t_{n+1}}^{-1}\dot{\boldsymbol{\eta}}_{r_{t_{n+1}}} + J_{t_{n+1}}^{-1}K_p\overset{\frown}{\boldsymbol{\eta}}_{t_{n+1}} + a_1(\mathbf{G}_{t_n} + M^{-1}\boldsymbol{\tau}_n) + \\ & \left. + \sum_{i=2}^{s} a_s(\mathbf{G}_{t_{n-s+1}} + M^{-1}\boldsymbol{\tau}_{n-s+1}) + \boldsymbol{\varepsilon}_{v_{n+1}}\right]^2 - \\ & - \overset{\frown}{\mathbf{v}}_{t_n}^T\overset{\frown}{\mathbf{v}}_{t_n}.\end{aligned} \tag{19}$$

For the sake of simplicity in the notation, the inner product for vectors $\mathbf{x}^T\mathbf{x}$ was indicated as $\mathbf{x}^2$.

The control action $\boldsymbol{\tau}_n$ can be decomposed into two components

$$\boldsymbol{\tau}_n = \boldsymbol{\tau}_{n_1} + \boldsymbol{\tau}_{n_2}, \tag{20}$$

with the first one designed as

$$\begin{aligned}\boldsymbol{\tau}_{n_1} = M\left(\right. & -K_v\overset{\frown}{\mathbf{v}}_{t_n} + \frac{1}{a_1}\left(-J_{t_n}^{-1}\dot{\boldsymbol{\eta}}_{r_{t_n}} + \right. \\ & + J_{t_{n+1}}^{-1}\dot{\boldsymbol{\eta}}_{r_{t_{n+1}}} - J_{t_{n+1}}^{-1}K_p\overset{\frown}{\boldsymbol{\eta}}_{t_{n+1}} + J_{t_n}^{-1}K_p\overset{\frown}{\boldsymbol{\eta}}_{t_n}\Big) + \\ & \left. - \sum_{i=1}^{s}\frac{a_s}{a_1}\left(\mathbf{G}_{t_{n-s+1}} + M^{-1}\boldsymbol{\tau}_{n-s+1}\right) - \mathbf{G}_{t_n}\right),\end{aligned} \tag{21}$$

with $K_v = K_v^T \geq 0$ another design matrix with K_p. It is noted that this component cancels almost all the terms in the kinematics path error $\overset{\frown}{\mathbf{v}}_{t_{n+1}}$.

Now the second component $\boldsymbol{\tau}_{n_2}$ will result from solving (19) with (21)

$$\begin{aligned}\Delta Q_{t_n} = {} & \\ & a\left(M^{-1}\boldsymbol{\tau}_{n_2}\right)^T M^{-1}\boldsymbol{\tau}_{n_2} + \mathbf{b}^T M^{-1}\boldsymbol{\tau}_{n_2} + c + \\ & + \overset{\frown}{\boldsymbol{\eta}}_{t_n}^T a_1 K_p\left(a_1K_p - 2I\right)\overset{\frown}{\boldsymbol{\eta}}_{t_n} + \\ & + \overset{\frown}{\mathbf{v}}_{t_n}^T a_1 K_v\left(a_1K_v - 2I\right)\overset{\frown}{\mathbf{v}}_{t_n} + \\ & + F(\boldsymbol{\varepsilon}_{\eta_{n+1}}, \boldsymbol{\varepsilon}_{v_{n+1}}),\end{aligned}$$

with

$$a = a_1^2 \tag{23}$$

$$\mathbf{b}^T = 2a_1\left(\left(I - a_1K_v\right)\overset{\frown}{\mathbf{v}}_{t_n}\right)^T \tag{24}$$

$$\begin{aligned}c = {} & a_1^2\left(J_{t_n}\overset{\frown}{\mathbf{v}}_{t_n} + \dot{\boldsymbol{\eta}}_{r_{t_n}} + \sum_{i=2}^{s}\frac{b_i}{a_1}J_{t_{n-i+1}}\mathbf{v}_{t_{n-i+1}}\right)^2 \\ & + a_1\left(J_{t_n}\overset{\frown}{\mathbf{v}}_{t_n} + \dot{\boldsymbol{\eta}}_{r_{t_n}}\right)^T\left(\boldsymbol{\eta}_{r_{t_n}} - \boldsymbol{\eta}_{r_{t_{n+1}}}\right) + \\ & + \left(\boldsymbol{\eta}_{r_{t_n}} - \boldsymbol{\eta}_{r_{t_{n+1}}}\right)^T\left(\boldsymbol{\eta}_{r_{t_n}} - \boldsymbol{\eta}_{r_{t_{n+1}}}\right) + \\ & + 2\left(I - a_1K_p\right)\overset{\frown}{\boldsymbol{\eta}}_{t_n}\left(a_1\left(J_{t_n}\overset{\frown}{\mathbf{v}}_{t_n} + \dot{\boldsymbol{\eta}}_{r_{t_n}}\right) + \right. \\ & \left. + \left(\boldsymbol{\eta}_{r_{t_n}} - \boldsymbol{\eta}_{r_{t_{n+1}}}\right)\right),\end{aligned} \tag{25}$$

and the vector function F fulfilling $F(\boldsymbol{\varepsilon}_{\eta_{n+1}}, \boldsymbol{\varepsilon}_{v_{n+1}}) \to 0$ when $h \to 0$.

Now, if there exist real roots of the polynomial $a\left(M^{-1}\boldsymbol{\tau}_{n_2}\right)^T M^{-1}\boldsymbol{\tau}_{n_2} + \mathbf{b}^T M^{-1}\boldsymbol{\tau}_{n_2} + c$, then the conditions for $\Delta Q_{t_n} < 0$, at least in an attraction domain equal to

$$\mathcal{B} = \left\{\overset{\frown}{\boldsymbol{\eta}}_{t_n}, \overset{\frown}{\mathbf{v}}_{t_n} \in \mathcal{R}^6 \cap \mathcal{B}_0\right\}, \tag{26}$$

with $\mathcal{B}_0 = \left\{\overset{\frown}{\boldsymbol{\eta}}_{t_n}, \overset{\frown}{\mathbf{v}}_{t_n}/\Delta Q_{t_n} \geq 0\right\}$ a residual set around zero , are the following

$$\frac{2}{a_1}I > K_p \geq 0 \tag{27}$$

$$\frac{2}{a_1}I > K_v \geq 0. \tag{28}$$

The residual set $\mathcal{B}_0$ depends clearly on $\boldsymbol{\varepsilon}_{\eta_{n+1}}$ and $\boldsymbol{\varepsilon}_{v_{n+1}}$, and it becomes the null point at the limit when $h \to 0$. The real roots are

$$\boldsymbol{\tau}_{n_2} = \frac{-M}{2a}\mathbf{b} \pm \frac{M}{2a}\sqrt{\frac{\mathbf{b}^T\mathbf{b} - 4ac}{6}}\mathbf{o}, \qquad (29)$$

with $\mathbf{o}$ a vector with all the six elements equal to one. In order to achieve minimal energy of the control action or eventually to avoid saturation, one can choose the solution $\boldsymbol{\tau}_{n_2}$ of the pair with minimal norm.

Finally, the complete control action is implemented at each discrete time by calculating $\boldsymbol{\tau}_n = \boldsymbol{\tau}_{n_1} + \boldsymbol{\tau}_{n_2}$.

6 Switching Controller

If, on the contrary, there are no real roots of the polynomial $a\left(M^{-1}\boldsymbol{\tau}_{n_2}\right)^T M^{-1}\boldsymbol{\tau}_{n_2} + \mathbf{b}^T M^{-1}\boldsymbol{\tau}_{n_2} + c$ in (22) because $4ac > \mathbf{b}^T\mathbf{b}$, one can choose the real part of (29), it is

$$\boldsymbol{\tau}_{n_2} = \frac{-M}{2a}\mathbf{b}, \qquad (30)$$

which gives the minimal value of (22) in the case of complex root given by

$$\begin{aligned}\Delta Q_{t_n} = c - \left((I - a_1K_v)\overset{\frown}{\mathbf{v}}_{t_n}\right)^2 - \qquad (31)\\ -\overset{\frown}{\boldsymbol{\eta}}_{t_n}^T a_1K_p\left(2I - a_1K_p\right)\overset{\frown}{\boldsymbol{\eta}}_{t_n} -\\ -\overset{\frown}{\mathbf{v}}_{t_n}^T a_1K_v\left(2I - a_1K_v\right)\overset{\frown}{\mathbf{v}}_{t_n} + F(\boldsymbol{\varepsilon}_{\eta_{n+1}}, \boldsymbol{\varepsilon}_{v_{n+1}}),\end{aligned}$$

with the quantity $c > \left((I - a_1K_v)\overset{\frown}{\mathbf{v}}_{t_n}\right)^2$ and K_p and K_v satisfying (27)-(28). The suboptimal $\boldsymbol{\tau}_{n_2}$ could still provide a large attraction domain with a appropriate selection of K_p and K_v, however with a larger residual set $\mathcal{B}_1$ than $\mathcal{B}_0$.

In fact the stability in this case will also depend on the sampling time h or equivalently on $a_1 = c_s h$, with c_s a constant depending on s (see models in (4)-(7)). As can be analyzed from (24) and (25), there is a sufficiently small h so that the positive difference $c - \left((I - a_1K_v)\overset{\frown}{\mathbf{v}}_{t_n}\right)^2$ be smaller that the negative definite terms (31). Also the term $F(\boldsymbol{\varepsilon}_{\eta_{n+1}}, \boldsymbol{\varepsilon}_{v_{n+1}})$ is insignificant for smaller h.

Even more important is the fact that a good selection of the design matrix K_v can be favorable to the appearance of real solutions (29). In this respect, one can see from (24) that $K_v = \frac{I}{a_1}$ would be the worst selection because $\mathbf{b} = \mathbf{0}$ and only the solution (29) could be implemented constantly. So K_v has to fulfill

$$\frac{2}{a_1}I > K_v > \frac{1}{a_1}I \qquad (32)$$

$$\frac{1}{a_1}I > K_v \geq 0. \qquad (33)$$

In view of that the law (29) is optimal with a smaller residual set $\mathcal{B}_0$ than that of the suboptimal law (30), and that the double scenario of real and complex roots can arise from time to time, the best control algorithm could be then built up as a switching control generating $\boldsymbol{\tau}_n = \boldsymbol{\tau}_{n_1} + \boldsymbol{\tau}_{n_2}$ with $\boldsymbol{\tau}_{n_1}$ as in (21) and $\boldsymbol{\tau}_{n_2}$ as in (29) for real roots or, alternatively, (30) for complex roots.

In view of the proposed switching controller, it is expected that the evolution of the control action $\boldsymbol{\tau}_n$ be jerky when the paths remain close to their references. This scenario is confirmed by numerical simulations that describe an alternation between solutions (29) and (30) in the neighborhood of the residual sets.

Finally, it is noticing that the increment of the order s of the Adams-Bashforth model entails the linear increment in the number of terms in $\boldsymbol{\tau}_{n_1}$ and $\boldsymbol{\tau}_{n_2}$, however they enter in the expressions as additive terms which simplifies the analysis of both the controller design and stability, and also the computation of $\boldsymbol{\tau}$ significantly. The choice of s can be done bearing in mind the quality of the model; yet the most simple model, $s = 1$, can be viable for small h.

7 Case Study

In order to illustrate the features of our control algorithm, let us consider the path tracking problem for the same vehicle used in Section IV. The vehicle has to navigate along a geometric path shown in Fig. 1 with a prescribed kinematics in time. The digital control algorithm is implemented according to (20). The sample time h was chosen 0.1 sec. and the simplest Adams-Bashforth model of $s = 1$ was employed.

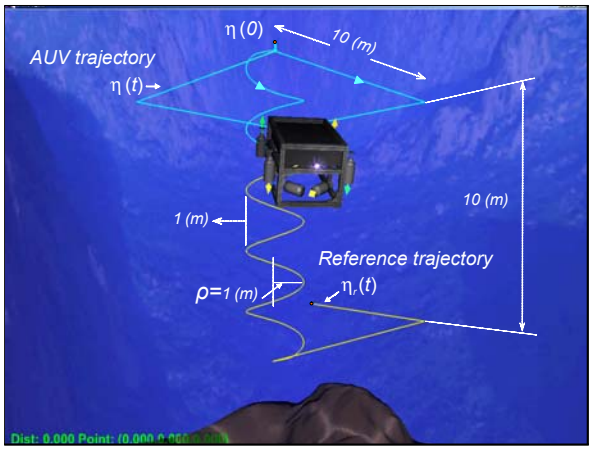

Figure 1. Path tracking problem for a subaquatic vehicle in 6 DOF.

In Figs. 2 and 3 all the state vector elements of $\boldsymbol{\eta}$, namely $x, y, z, \varphi, \theta, \psi$, and of $\mathbf{v}$ namely u, v, w, p, q, r are depicted comparatively together with the evolution of their respective references. One notices on the right hand of this pictures that the transient phase elapses a short period of about 5 sec. During the whole navigation period optimal and suboptimal solutions for the control action have taken place with alternation, above all in the stationary state when the path tracking errors were small. So, the residual set has resulted minimal and was given by the sampled-data model errors of the order of magnitude of about 10^{-4} (see Table I for $h = 0.1$ sec. and $s = 1$).

Generally speaking, the all-round performance of the control system is very good and comparable with the analogous control obtained at the limit for $h \to 0$ [Jordán and Bustamante, 2007].

8 Conclusions

In this paper outstanding features of numeric methods based on Adams-Bashforth approximations were exploited for sampled-data modeling of a large class of vehicle dynamics in many degrees of freedom. The

sampled-data models contain the original physical matrices of the underlying ODEs of the vehicle dynamics which make them quite appropriate to translate available analogous controller designs to digital counterparts. Afterwards, the problem of path tracking and regulation with geometric and kinematic specifications on the reference paths was focused. An approach to model-based controller design was presented based on a Lyapunov method over an incremental functional of the path error energies. It is proved that the asymptotic convergence can be ensured for small sampling periods up to a residual set whose measure depends only on the one-step-ahead sampled-data model errors. Future works consider the analysis of the algorithm robustness when noise perturbations are included in the system.

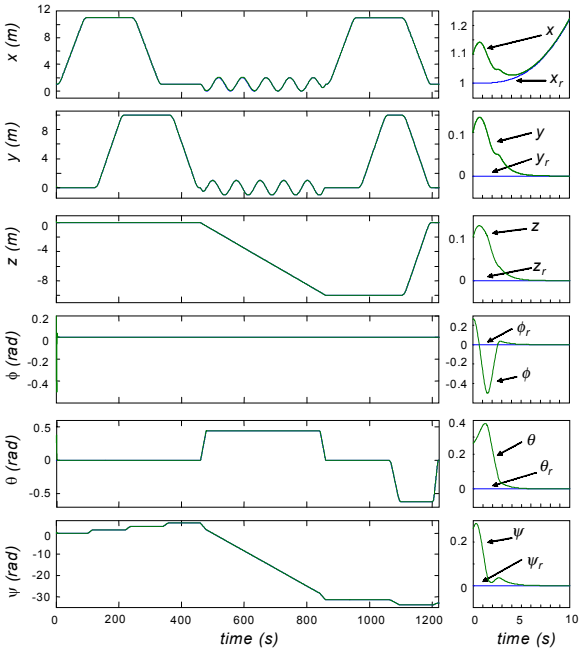

Figure 2. Evolution of the position variables.

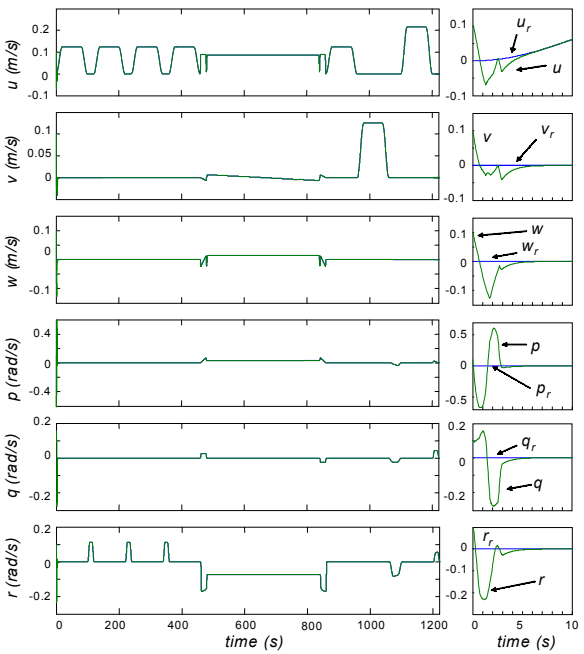

Figure 3. Evolution of the kinematic variables.

Design matrices for independently tuning of the kinematic and geometric path tracking are provided. They can be optimally selected in order for both the stability of the controller and a good transient performance to be achieved. A case study for a 6 degrees-of-freedom vehicle using Adams-Bashforth models with different sampling times and orders was presented. Then the features of the proposed digital controller were illustrated for the same case by means of numerical simulations.

References

Albertos, P. (1996). Sampled-data Modeling and Control of Nonlinear Systems. In *35th IEEE Conf. on Decision and Control,* Kobe, Japan, pp. 925-930.

Butcher, J. C. (2003). *Numerical Methods for Ordinary Differential Equations.* John Wiley and Sons. Chistester, England.

Cunha, J. P. V. S, Costa, R. R. and Hsu, L. (1995) Design of a High Performance Variable Structure Position Control of ROV's. *IEEE J. of Oceanic Engineering*, **20**(1), pp. 42-55.

Fossen, T. I. (1994). *Guidance and Control of Ocean Vehicles*. John Wiley&Sons. New York.

Hairer, H., Nørsett, S. P. and Wanner, G. (1987). *Solving Ordinary Differential Equation I*. Springer. New York.

Jordán, M. A. and Bustamante, J. L. (2007). On the Presence of Nonlinear Oscillations in the Teleoperation of Underwater Vehicles Under the Influence of Sea Wave And Current. In *2007 American Control Conference*, New York , USA, July 11-13, 2007, pp. 894-899.

Jordán, M. A. and Bustamante, J. L. (2008) Guidance of Underwater Vehicles with Cable Tug Perturbations Under Fixed and Adaptive Control Modus. *IEEE J. of Oceanic Engineering*, **33**(4), pp. 579 - 598.

Jordán, M. A. and Bustamante, J. L. (2009). Modular Modeling of Complex Dynamics with Adams-Bashforth Sampled-Data Models for Control Purposes. In *10th Argentine Symposium on Computing Technology (AST 2009)*, Mar del Plata, Argentina, August 24-25, 2009.

Nĕsic, D., Teel, A. R. and Sontag, E. D. (1999) Formulas relating KL stability estimates of discrete-time and sampled-data nonlinear systems. *Syst. Contr. Lett.*, **38**, pp. 49-60.

Nĕsic, D. and Teel, A.R. (2004) A framework for stabilization of nonlinear sampled-data systems based on their approximate discrete-time models. *IEEE Trans. Automat. Contr.*, **49**, pp. 1103-1034.

Smallwood, D. A. and Whitcomb, L. L. (2003) Adaptive Identification of Dynamically Positioned Underwater Robotic Vehicles," *IEEE Trans. on Control Syst. Technology*, **11**(4), 2003, pp. 505-515.

Yuz, J. I. and Goodwin, G. C. (2005) On sampled-data models for nonlinear systems. *IEEE Trans on Automatic Control*, **50** (10), pp. 1477-1488.